Δελτίο της Ελληνικής Γεωλογικής Εταιρίας, τομ. XLVII , 2013 Πρακτικά 13ου Διεθνούς Συνεδρίου, Χανιά, Σεπτ. 2013	Bulletin of the Geological Society of Greece, vol. XLVII 2013 Proceedings of the 13th International Congress, Chania, Sept. 2013

THE 10 JUNE 2012 MW6.0 EARTHQUAKE SEQUENCE IN THE EASTERNMOST END OF THE HELLENIC ARC

Kiratzi A.[1], Aktar M.[2] and Svigkas N.[1]

[1] *Department of Geophysics, Aristotle University of Thessaloniki, Greece*

[2] *Kandilli Observatory and Earthquake Research Institute, Bogaziçi University, Istanbul, Turkey*

Abstract

The 10 June 2012 (UTC 12:44:17.3; lat. 36.441°N, long. 28.904°E, Mw6.0) earthquake sequence, 60 km to the west of Rodos Island, is studied, in an attempt to shed light to the obscure deformation pattern at the easternmost end of the Hellenic Arc. Moment tensor solutions for the mainshock and the strongest aftershocks revealed the operation of WNW-ESE dextral strike-slip faulting, with slip vector at ~N295°E, approximately orthogonal to the GPS velocity vectors. The strike of the activated structure generally aligns with bathymetric linear escarpments observed in the region, bordering the eastern section of the Rodos basin. The best constrained focal depths are in the range 10 to 25 km, with the mainshock at the depth of 24 km. The slip model for the mainshock, obtained through a finite-fault inversion scheme, showed that slip was mainly concentrated in a single patch, with the locus of peak slip (~125 cm) located ~ 4km to the NW of the hypocenter. The sequence which lies in the western continuation of the Fethiye – Burdur sinistral strike-slip zone into the Aegean Sea and Rodos basin, is not connected with activation of this zone. Its characteristics comply with the activation of a dextral strike-slip structure, oblique to this zone, which accommodates along – arc NE-SW extension.
Key words: *Rodos Basin; slip model; rupture; focal mechanism.*

Περίληψη

Μελετάται η σεισμική ακολουθία της 10ης Ιουνίου 2012 (UTC 12:44:17.3; 36.441°B; 28.904°E, Mw6.0), 60 χιλιόμετρα δυτικά της Ρόδου, στο ανατολικότερο άκρο του ελληνικού τόξου. Οι μηχανισμοί γένεσης του κύριου σεισμού και των ισχυρότερων μετασεισμών έδειξαν τη λειτουργία ενός ΔΒΔ-ΑΝΑ ρήγματος δεξιόστροφης οριζόντιας συνιστώσας, με διάνυσμα ολίσθησης ~Β295°Α. Η παράταξη της δομής που ενεργοποιήθηκε ακολουθεί την τοπογραφία του βυθού στην ευρύτερη περιοχή του ανατολικού τμήματος της λεκάνης της Ρόδου. Τα καλύτερα προσδιορισμένα εστιακά βάθη κυμαίνονται από 10 έως 25 χλμ, με την εστία του κύριου σεισμού στον κατώτερο φλοιό, σε βάθος 24 χιλιομέτρων. Το μοντέλο ολίσθησης για τον κύριο σεισμό, έδειξε ότι η ολίσθηση στην επιφάνεια του ρήγματος είναι συγκεντρωμένη σε ένα μεμονωμένο τμήμα. με το μέγιστο της τιμής της να είναι ~ 125 εκατοστά. Το μέγιστο δεν εμφανίζεται στο υπόκεντρο, αλλά ~4 χλμ στα βορειοδυτικά αυτού. Η σεισμική ακολουθία του Ιουνίου 2012 βρίσκεται στην δυτική συνέχεια της αριστερόστροφης ζώνης Fethiye – Burdur προς την πλευρά του Αιγαίου Πελάγους και της λεκάνης της Ρόδου. Εντούτοις, ο σεισμός του Ιουνίου 2012 δεν συνδέεται με την ενεργοποίηση αυτής της ζώνης, ούτε συνηγορεί για την προς δυσμάς συνέχειά της. Τα

χαρακτηριστικά της ακολουθίας δείχνουν την ενεργοποίηση ενός δεξιόστροφου ρήγματος οριζόντιας μετατόπισης, με πλάγια παράταξη ως προς τη ζώνη, που απορροφά εφελκυσμό παράλληλα προς το ελληνικό τόξο κατά διεύθυνση ΒΑ-ΝΔ.
Λέξεις κλειδιά: *Μοντέλο ολίσθησης, Λεκάνη Ρόδου, διάρρηξη, μηχανισμός γένεσης.*

1. Introduction

The Hellenic Subduction Zone has a significant role in the active tectonic pattern of Eastern Mediterranean Sea. It is formed from the subduction of Mesozoic African lithosphere beneath the overriding Aegean Sea material. Africa is moving north towards Eurasia at only 5 to 10 mm/year, whereas the Aegean is moving faster to the south-west with respect to Eurasia, resulting in about 35 mm/yr that have to be accommodated by deformation along the Hellenic Subduction zone. The eastern border of the Hellenic Trench, close to the coastal regions of western Anatolia, is poorly studied, mainly due to the insufficient number of strong events.

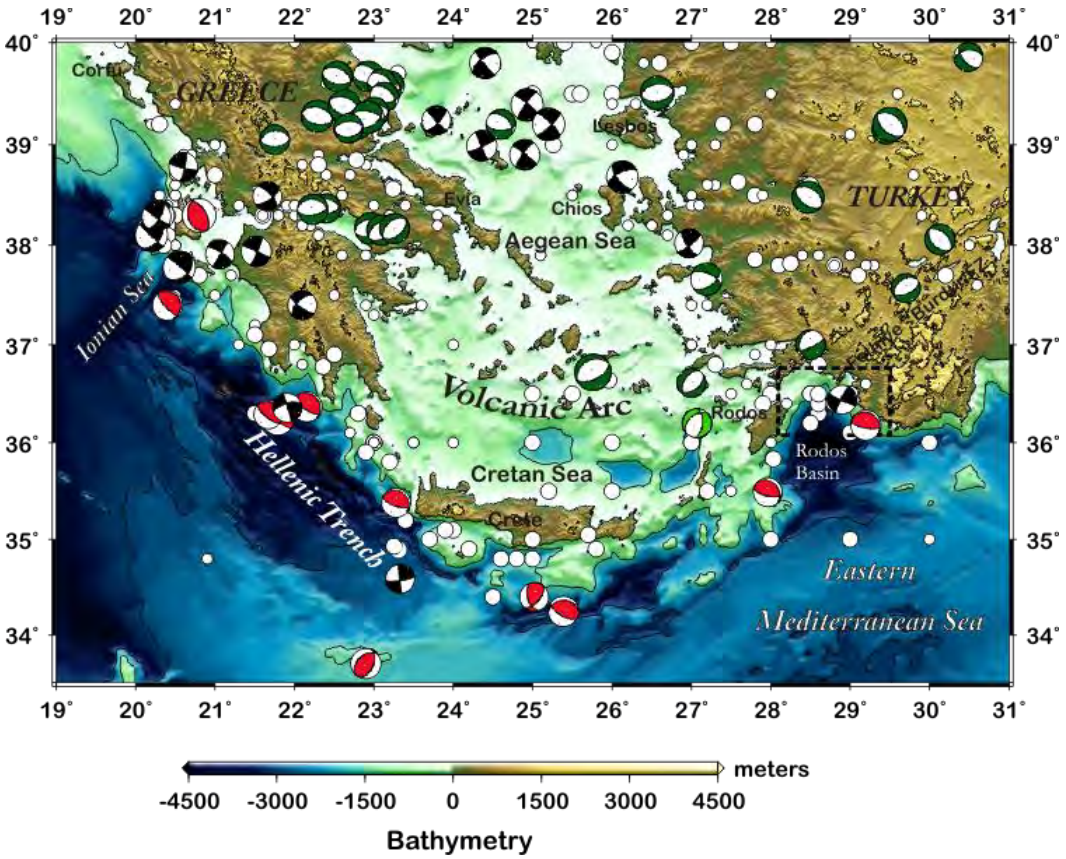

Figure 1 - The location of the 10 June 2012 sequence, marked with the dashed rectangle, at the easternmost section of the Hellenic Subduction Zone. The colour beach- balls (from Kiratzi and Louvari, 2003; Kiratzi et al., 2007) denote the available focal mechanisms for previous events with Mw>6.0. The seismicity of the period 550BC- 2012 with M>6.0 is also plotted (open circles).

The 10 June 2012 earthquake sequence occurred offshore and in the mid-distance between the Island of Rodos and the city of Fethiye in south-western Anatolia (Figure 1). From the Turkish side the broader region of occurrence is dominated by the presence of the transtensional left-lateral Fethiye - Burdur Fault Zone (FBFZ). It is a well known structure of pronounced NE-SW trending

faults and basins, which roughly align between the cities of Fethiye and Afyon (Taymaz and Price, 1992; Ocakoğlu, 2012). These faults are combined with N-S faults, to form an en-echelon basin configuration, which continues westward into the eastern Hellenic Arc. The sinistral strike-slip character of the FBFZ is mainly indicated by the analysis of structural data and of sediment deposits. More specifically, structural analyses on the Turkish coastal regions suggest that the Holocene – Recent deformation was taken up in a transtensional environment which required the progressive addition of a sinistral shear motion, to confront the NE propagating transcurrent motion of the Hellenic fore-arc (ten Veen, 2004).

To this end, the 10 June 2012 earthquake occurred in a region, of interaction between the western prolongations of the Fethiye – Burdur Fault Zone and the Hellenic Subduction. The sequence is studied here, in terms of the focal mechanisms, the time and space evolution and the slip model of the mainshock. The data for this study were derived from the broad band stations of the Greek and Turkish stations, thus providing a good coverage in most azimuths, except a gap in coverage in the southeast.

2. Moment Tensor (MT) Solutions and Relocation of Aftershocks

2.1 MT Inversions

Moment tensors of the mainshock and of the stronger events of the sequence were computed by the Time-Domain Moment Tensor inversion method (Dreger, 2003). The method is now routinely applied and for its applications in the Aegean Sea region the details are described in Roumelioti et al. (2010). We solved for the deviatoric seismic moment tensor only.

Table 1 – Information on the focal mechanism solutions of the strongest events of the June 2012 sequence (VR= Variance Reduction of the solution; Nst= number of stations used in the inversion).

Date Y/MM/DD	Origin Time hh:mm:ss.s	Lat	Long	Depth km	Mw	NODAL PLANE 1 Strike°	Dip°	Rake°	NODAL PLANE 2 Strike°	Dip°	Rake°	VR %	Nst
20120610	12:44:17.3	36.468	28.888	24	6.0	115	85	171	206	81	5	78	9
20120610	15:02:41.1	36.464	28.873	15	3.3	295	78	-173	204	83	-12	56	3
20120610	18:28:33.9	36.448	28.895	16	3.9	153	88	175	243	85	2	73	4
20120611	02:06:35.9	36.400	28.970	22	3.8	307	87	-172	217	82	-3	84	7
20120611	17:35:39.1	36.422	28.973	30	3.8	123	89	177	213	87	1	85	3
20120611	19:51:06.8	36.429	28.948	14	3.7	163	82	174	254	84	8	50	3
20120614	16:46:07.7	36.390	29.020	25.0	4.5	310	86	-177	220	87	-4	83	6
20120625	13:05:30.0	36.457	28.916	20.0	4.7	143	82	172	234	82	8	80	5

The inversion yields the M_{ij} which is decomposed into the scalar seismic moment, a double-couple (DC) moment tensor and a compensated linear vector dipole (CLVD) moment tensor. The decomposition is represented as percent DC and percent CLVD. Source depth is found iteratively by finding the solution that yields the largest variance reduction. It is assumed that the event location is well represented by the high frequency hypocentral location, and a low frequency centroid location is not determined. Moreover, the representation assumes that the source time

history is synchronous for all of the moment tensor elements and that it may be approximated by a delta function. Finally, it is assumed that the crustal model is sufficiently well known to explain low frequency wave propagation.

To apply the method, broad band waveforms were retrieved from the Hellenic Unified Seismic Network (HUSN) and the Turkish network operated by the Kandilli Observatory (KOERI). Prior to the inversion, full broadband waveforms of the three recorded components were band-pass filtered between 0.02–0.08 Hz or 0.05-0.10 Hz depending on the magnitude of the event and the signal-to-noise ratio of the waveforms. Theoretical Green's functions required to model the propagation of the seismic waves were constructed with the method and code described by Saikia (1994) using the velocity model of Novotný et al. (2001), which has proven to successfully describe low frequency wave propagation (e.g., Roumelioti et al.,2010; Kiratzi, 2010, 2011 and references therein). In Figure 2 we show the moment tensor solution and the waveform fit for the mainshock, while the parameters of the computed focal mechanisms of the aftershocks are listed in

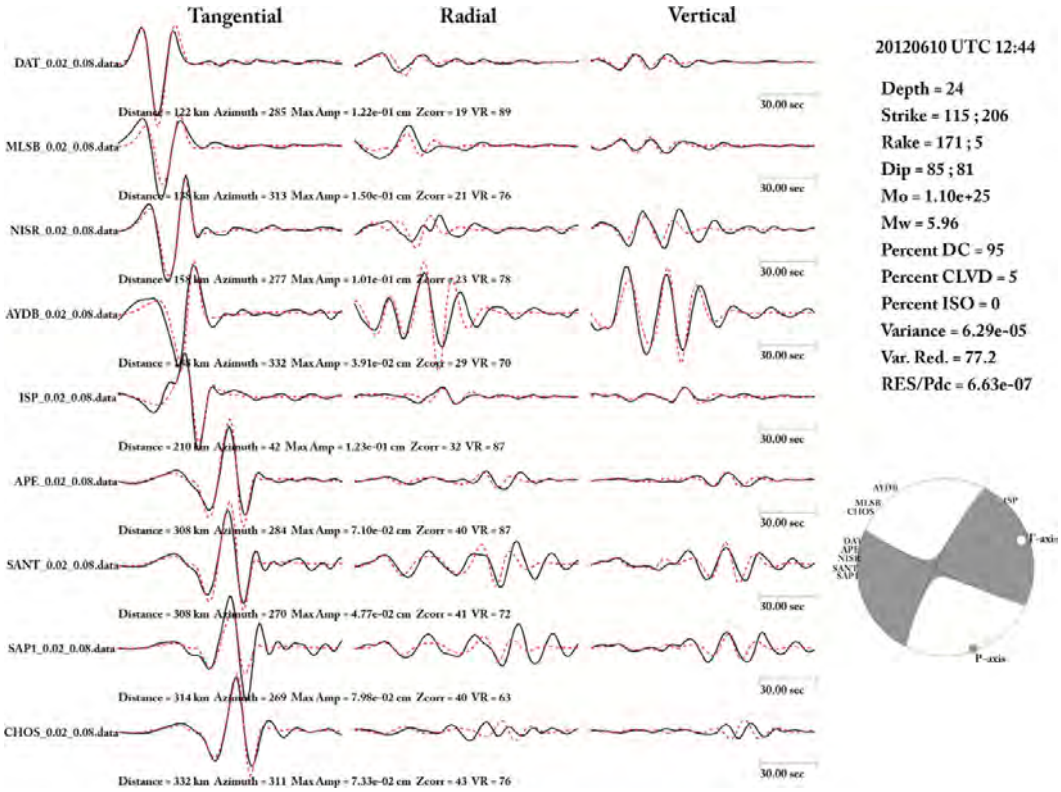

Figure 2 - Deviatoric moment tensor point-source inversion results for the 10 June 2012 mainshock using waveform data from the Greek and Turkish networks. For each station three component displacement seismograms (shown as solid lines) are compared to one-dimensional synthetic seismograms (dashed red lines), while the azimuth, the maximum three-component trace amplitude, cross-correlation samples (Zcorr) and Variance Reduction (VR) are also provided. The lower-hemisphere projection of the P-wave radiation pattern is shown at right, together with the azimuthal distribution of the stations included in the inversion. Solution information includes the strike, rake, and dip for the two possible double-couple planes, the scalar seismic moment, the moment magnitude, and percentage DC, CLVD. Fitting parameters as the variance, the variance reduction (Var. Red) and the variance modulated by the percent double-couple (RES/Pdc) are also given.

Table 1. Our solution is in very good agreement with those published by other agencies, as these can be retrieved from the site of the EMSC (http://www.emsc-csem.org).

2.2 Relocation Results

The strongest events of the sequence have already occurred by mid July 2012. More specifically the mainshock on 10 June 2012 (UTC 12:44:16.73) was followed within minutes by the strongest aftershock of Mw4.8 (UTC 12:49:36.97). Unfortunately, for this aftershock a moment tensor solution is not provided, because the waveforms were mixed with the coda of the mainshock.

In order to relocate the epicentres we joined phase data from the Greek and Turkish stations. We read ourselves P and S phases from the closest stations, particularly the S arrivals, in an attempt to increase the depth resolution. We used HypoDD (Waldhauser and Ellsworth, 2000) and LSQR for the relocation; from the initial set of 65 events, we were able to relocate a subset of 51 events with M>2.0, which passed the criteria. Our relocation was combined with waveform cross-correlation for the closest stations. Our relocated dataset is complete for M>2.6, e.g. including 42 events in total. Using the utilities of ZMAP we obtained a b –value equal to 0.61.

The distribution of the best located events, shown in Figure 3 and in cross-section in Figure 4, show a number of interesting features. From a close inspection of the aftershock cloud it is immediately noticed that the activated structure has a NW-SE trend, implying that from the two nodal planes of the focal mechanism, the NW-SE trending plane is the fault plane. The mainshock occurred at the northernmost cloud and within minutes the strongest aftershock occurred at the southern cloud, with most of the aftershocks located at that cloud. The length of the activated structure is about 9 Km, in accordance with the predictions of empirical scaling relations for an Mw6.0 earthquake. It is worth noting also (Figure 4) that the majority of the aftershock activity is concentrated at shallower depths (<15 km) compared to the mainshock and strongest aftershocks (>20 km), an observation previously made in the case of Adana 1998 sequence, located similarly next to an active subduction zone in Eastern Mediterranean Sea (Aktar et al., 2000).

3. Distribution of Slip onto the Fault Plane

3.1 Method

To obtain the slip distribution onto the ruptured fault plane for the 10 June 2012 mainshock the finite-fault inversion method of Kaverina et al. (2002), a nonnegative, least-squares scheme with simultaneous smoothing and damping was applied. The same code can be used to simulate ground motions from a slip model.

In brief, this method inverts for fault slip distributed over a grid of point sources that are triggered according to the passage of a circular rupture front. A Laplacian-smoothing operator, slip positivity, and a scalar moment minimization constraint is applied to stabilize the inversions. Green's functions based on the Novotný et al. (2001) velocity profile, shown to be effective in modelling regional wave propagation, were used to invert the seismic waveforms, and were calculated using the frequency–wavenumber integration method (Saikia, 1994) for 1-km intervals in distance and 1-km intervals in depth. The source model used is a single fault plane with constant rupture velocity and constant dislocation rise time.

3.2 Application Results

The seismic data consist of three component broad band displacement waveforms recorded at regional stations of the Greek and neighbouring networks. Both the data and the synthetic Green's functions were bandpass filtered between 0.02 to 0.08 Hz. From a standard grid search of the parameter space, the rupture velocity was found to be 2.9 km/s and the rise time 0.5 s.

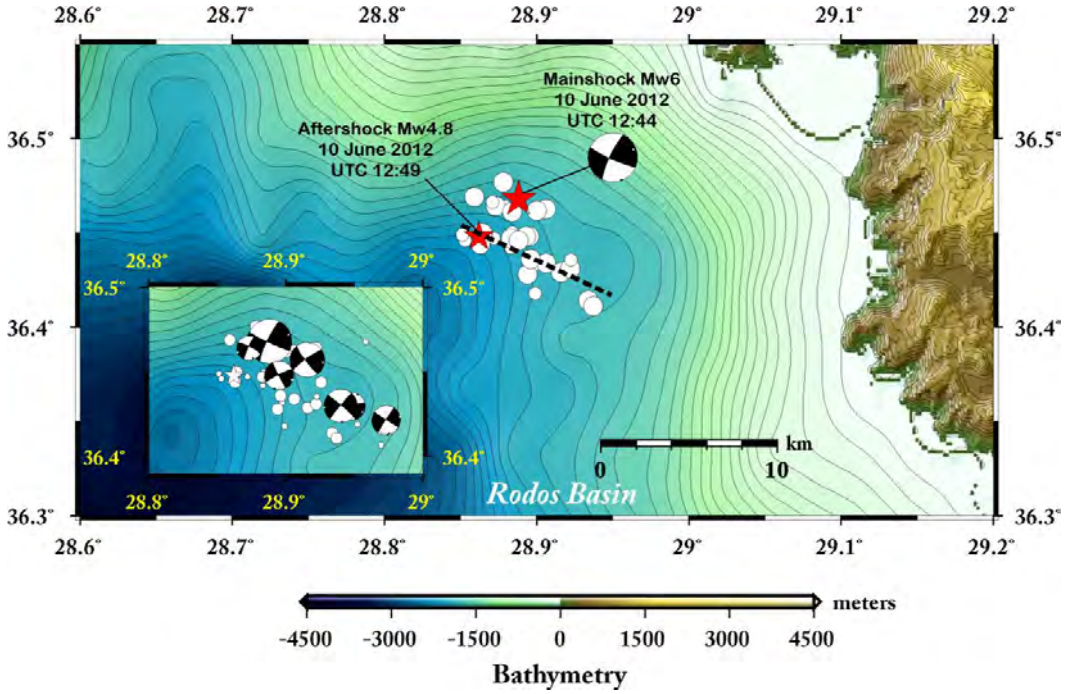

Figure 3 - HypoDD relocated epicentres of the June 2012 sequence, together with the focal mechanism of the mainshock for comparison. Note that the cloud of aftershocks clearly denotes the NW-SE nodal plane as the fault plane. The dashed line is parallel to the fault plane to visually show this. The inset to the left shows the focal mechanisms of the stronger aftershocks computed by moment tensor inversion (listed in Table 1).

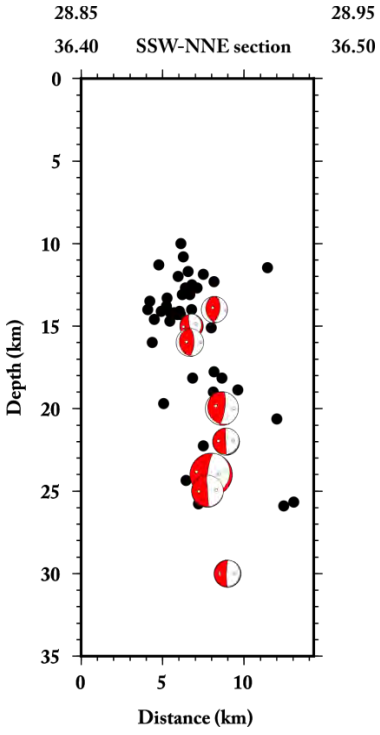

Figure 4 - Cross-section along a plane perpendicular to the fault plane (coordinates shown on top of the section), to show that the sequence operated in the depth range 10 to about 25 km, with the majority of the aftershocks in the range 10 to 15 km.

The results of the inversion show that slip is confined in a main patch, and the maximum slip is located ~4 km to the WNW of the hypocenter location (Figure 5), providing evidence for a mainly unilateral rupture to NW. A deeper patch of slip is also observed to the SE of the hypocenter, at a depth of ~32 Km that fits large lapse time signal in the data. This patch was a stable feature in all trial inversions, and is not very likely to be an artifact. Average slip in the ruptured area is ~19 cm and peak slip reaches 125 cm. The total scalar seismic moment for the slip model is M_o=1.80x10^{25} dyn-cm, resulting in moment magnitude Mw6.1, slightly larger than the Mw obtained in the moment tensor solution (Figure 2).

The total data variance reduction for the solution, calculated as a normalized squared misfit, is 85%, indicating a very satisfactory level of fit, between observed and slip-model produced synthetic waveforms, which are shown in Figure 6.

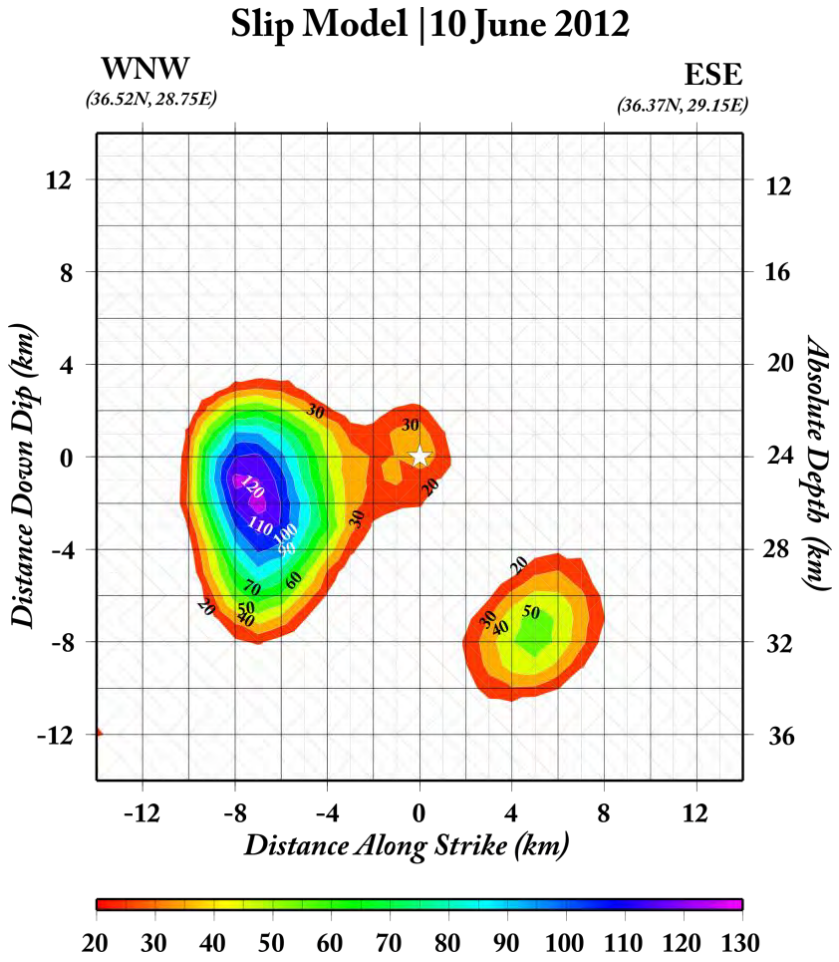

Figure 5. Slip model for the event of 10 June 2012 Mw6.0 event obtained from the inversion of broad band waveforms, for the N115°E trending fault plane, adopting a rupture velocity of 2.9 km/s, found from a standard grid search of the parameter space. One main slip patch is calculated where the peak slip value (~125 cm) was observed, with approximate dimensions 5x5 km². The asterisk denotes the hypocentre location, which lies at an absolute depth of 24 km. Note that the locus of slip is concentrated ~ 4 km to the NW of the hypocenter, and if directivity is present, it should be in that direction. A second slip patch is also observed, which is deeper than the previous and less pronounced, but which was a stable feature in all test inversions and fits the long lapse time in the data.

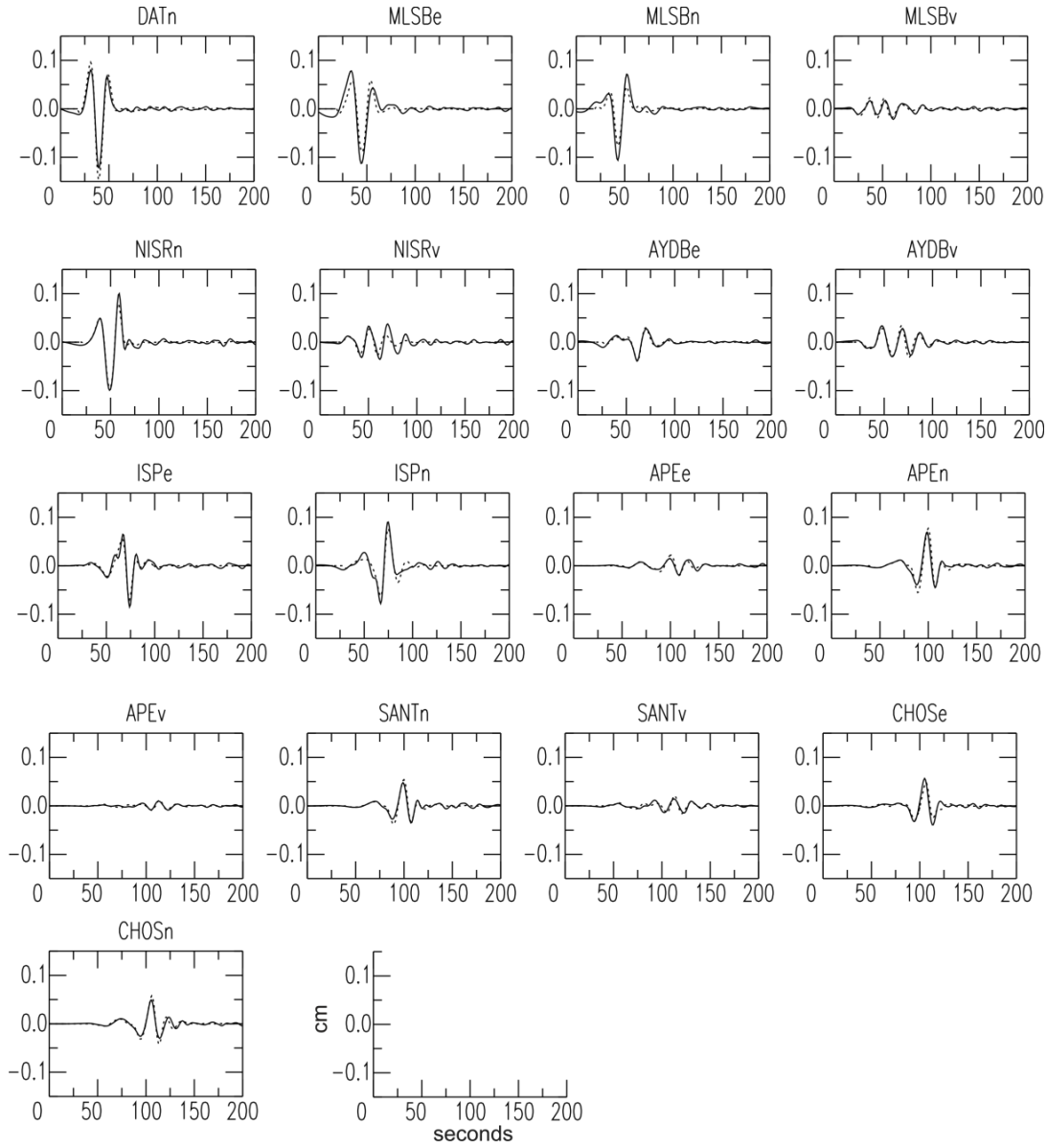

Figure 6. Comparison of observed (straight lines) and of synthetic (dashed lines) waveforms. Synthetics were calculated using the slip model for mainshock of 10 June 2012 Mw6.0 (Fig. 5). The fit in most of the stations is very good, resulting in a large Variance Reduction (85%) for the inversion.

4. Conclusions

The eastern termination of the Hellenic Subduction Zone is insufficiently studied compared to its western and central part, mainly due to the lack of strong earthquakes to be instrumentally recorded by the present seismological networks in Greece and Turkey (Shaw and Jackson, 2010; Shaw, 2012). The 10 June 2012 event Mw6.0 with an epicentre in the mid distance between Rodos Island and the city of Fethiye in coastal western Anatolia was studied in an attempt to shed light to

the seismotectonic features of the region. Moment tensor solutions of the mainshock and of the strongest aftershocks revealed the operation of strike-slip faulting in the region, in the depth range 10 to 25 km, while the strongest events nucleated at the lower crust. The HypoDD relocated epicentres of the sequence led to the identification of the fault plane, which strikes NNW-ESE (N115°E) indicating dextral strike-slip motion. The 2012 sequence is located in the western prolongation of the Fethiye – Burdur Fault Zone (FBFZ) towards the Aegean Sea and Rodos Basin. This zone is considered to be connected with sinistral strike-slip faulting. To this end, the sequence studied here is not connected with this zone, neither does it support its western extension, but on the contrary it involves rupture of a rather deep strike-slip fault that is oblique to the FBFZ (see Fig. 1), in a sense reflecting the interaction of Africa – Anatolia lithospheres at their easternmost sections.

Finite – fault inversion applied to broad band displacement waveforms of the Greek and Turkish networks, revealed that the slip onto the causative fault is concentrated at main patch of 5×5 Km². The locus of the peak slip which was calculated to be 125 cm is located 4 Km to the NNW of the hypocenter, providing evidence for rupture propagation mainly towards that direction. The average slip onto the fault plane is 19 cm and the resolved total seismic moment is 1.80×10^{25} dyn-cm. The obtained slip model provides very good fit to the observed waveforms.

The T-axes of the focal mechanisms of the 2012 sequence indicate extension approximately NE-SW in accordance with the regional stress field. This along-arc extensional field is characterising the entire region south of the Hellenic Volcanic Arc and is considered to be related to the outward growth of the Hellenic Arc in response to the westward Anatolia extrusion. In conclusion the 10 June 2012 Mw6.0 sequence is characterized by dextral strike-slip faulting associated with the activity of NW-SE trending faults that accommodate NE-SW extension, as observed in many regions south of the Hellenic Volcanic Arc (Benetatos et al., 2004; Kiratzi, 2012 and references therein).

5. Acknowledgments

This work was financed by TUBITAK of Turkey (Project Number: 109Y402) and the General Secretariat for Research & Technology (GSRT) of Greece (Project Number: 10 TUR/1-3-52) in the framework of the Turkey-Greece bilateral project with title: “Turkey – Greece cross border seismicity: velocity models, moment tensors, slip models, shake maps based on knowledge-transfer and a joint database repository”. AK also acknowledges co-finance by the European Union (European Social Fund – ESF) and Greek national funds through the Operational Program "Education and Lifelong Learning" of the National Strategic Reference Framework (NSRF) - Research Funding Program: Thales “Investing in knowledge society through the European Social Fund”. Broad band waveforms used in this study were retrieved from the Hellenic Unified Seismological Network of Greece, and the network operated by Kandilli Observatory in Turkey. Moment tensors were computed using the tdmt-invc_iso package developed by Douglas Dreger and Sean Ford of the Berkeley Seismological Laboratory, and Green’s functions were computed using the FKRPROG software developed by Chandan Saikia. Figures were produced using the General Mapping Tools software (Wessel and Smith, 1998). The SAC software (Goldstein and Snoke, 2005) was used to process the waveforms. Special thanks are extended to our colleagues Vasilis Karakostas, K. Leptokaropoulos and H. Garlaouni who provided many helpful scripts to manage the data.

6. References

Aktar M., Ergin M., Özalaybey S., Tapirdamaz C., Yörük A. and Biçmen F. 2000. A lower-crustal event in northeastern Mediterranean: the 1998 Adana earthquake (Mw=6.3) and its aftershocks, *Geophys. Res. Lett*., Vol. 27, N:16, 2361-2364.

Benetatos C., Kiratzi A., Papazachos C. and Karakaisis G. 2004. Focal mechanisms of shallow and intermediate depth earthquakes along the Hellenic Trench, *Journal of Geodynamics*, 37, 253-296.

Dreger D. S. 2003. TDMT_INV: Time Domain Seismic Moment Tensor INVersion, *International Handbook of Earthquake and Engineering Seismology*, Volume 81B, p 1627.

Goldstein P. and Snoke A. 2005. SAC Availability for the IRIS Community, Incorporated Institutions for Seismology Data Management Center Electronic Newsletter.

Kaverina A., Dreger D. And Price E. 2002. The Combined Inversion of Seismic and Geodetic Data for the Source Process of the 16 October 1999 Mw 7.1 Hector Mine, California, Earthquake, *Bulletin of the Seismological Society of America,* 92, 1266-1280.

Kiratzi A. 2010. The 24 May 2009 Mw5.2 earthquake sequence near Lake Doirani (FYROM - Greek borders): focal mechanisms and slip model using empirical Source Time Function's inversion, *Tectonophysics*, 490, 115-122.

Kiratzi A. 2011. The 6 September 2009 Mw5.4 earthquake in Eastern Albania – FYROM Border: focal mechanisms, slip model, ShakeMap, *Turkish Journal of Earth Sciences,* 20 (4), 475–488.

Kiratzi A. 2013. The January 2012 earthquake sequence in the Cretan Basin, south of the Hellenic Volcanic Arc: Focal mechanisms, rupture directivity and slip models, *Tectonophysics*, http://dx.doi.org/10.1016/j.tecto.2012.11.019

Kiratzi A. and Louvari E. 2003. Focal mechanisms of shallow earthquakes in the Aegean Sea and the surrounding lands determined by waveform modelling: a new database, *Journal of Geodynamics,* 36 (1–2), 251–274.

Kiratzi A., Benetatos C. and Roumelioti Z. 2007. Distributed earthquake focal mechanisms in the Aegean Sea, *Bulletin of the Geological Society of Greece*, Vol. XXXX, 1125-1137.

Novotný O., Zahradník J., and Tselentis G.A. 2001. North-Western Turkey earthquakes and the crustal structure inferred from surface waves observed in Western Greece, *Bulletin of the Seismological Society of America*, 91, 875-879.

Ocakoğlu N. 2012. Investigation of Fethiye-Marmaris Bay (SW Anatolia): seismic and morphologic evidences from the missing link between the Pliny Trench and the Fethiye-Burdur Fault Zone, *Geo-Marine Letters*, (2012) 32, 17–28.

Roumelioti Z., Kiratzi A. and Benetatos C. 2010. Time Domain Moment Tensors of Earthquakes in the broader Aegean Sea for the years 2006-2007: the database of the Aristotle University of Thessaloniki, *Journal of Geodynamics*, doi: 10.1016/j.jog.2010.01.011.

Saikia C. K. 1994. Modified frequency-wavenumber algorithm for regional seismograms using Filon's quadrature; modeling of Lg waves in eastern North America, *Geophysical Journal International*, 118, 142-158.

Shaw B. 2012. Active Tectonics of the Hellenic Subduction Zone, Springer Theses, 1, doi: 10.1007/978-3-642-20804-1_1, © *Springer-Verlag Berlin.*

Shaw B. and Jackson J. A. 2010. Earthquake mechanisms and active tectonics of the Hellenic subduction zone, *Geophysical Journal International*, 181 (2), 966-984.

Taymaz T. and Price S. 1992. The 1971 May 12 Burdur earthquake sequence, SW Turkey: a synthesis of seismological and geological observations, *Geophysical Journal International,* 108, 589-603.

Ten Veen J. 2004. Extension of Hellenic forearc shear zones in SW Turkey: the Priocene-Quaternary deformation of the Esen Cay Basin, *Journal of Geodynamics*, 37, 181-204.

Waldhauser F. and Ellsworth W. L. 2000. A double-difference earthquake location algorithm: Method and application to the northern Hayward fault, *Bull. Seismol. Soc. Am.,* 90, 1353–1368.

Wessel P. and Smith W.H.F. 1998. New improved version of the Generic Mapping Tools released, *EOS Transactions, AGU* 79, 579.